Inorg. Chem. **2005**, *44*, 7582–7589

Chelate Ring Size Variations and Their Effects on Coordination Chemistry and Catechol Dioxygenase Reactivity of Iron(III) Complexes†

Michael Merkel, Matthias Pascaly, and Bernt Krebs*

Institut für Anorganische und Analytische Chemie, Westfälische Wilhelms-Universität Münster, Wilhelm-Klemm-Strasse 8, 48149 Münster, Germany

Jörg Astner, Simon P. Foxon, and Siegfried Schindler*

Institut für Anorganische und Analytische Chemie der Justus-Liebig-Universität Giessen, Heinrich-Buff-Ring 58, 35392 Giessen, Germany

Received May 6, 2005

The catechol dioxygenase reactivity of iron(III) complexes using tripodal ligands was investigated. Increasing, as well as decreasing, chelate ring sizes in the highly active complex [Fe(tmpa)(dbc)]B(C_6H_5)$_4$ (tmpa = tris[(2-pyridyl)-methyl]amine; dbc = 3,5-di-*tert*-butylcatecholate dianion), using related ligands, only resulted in decreased reactivity of the investigated compounds. A detailed low-temperature stopped-flow investigation of the reaction of dioxygen with [Fe(tmpa)(dbc)]B(C_6H_5)$_4$ was performed, and activation parameters of $\Delta H^{\ddagger} = 23 \pm 1$ kJ mol^{-1} and $\Delta S^{\ddagger} = -199 \pm 4$ J mol^{-1} K^{-1} were obtained. Crystal structures of bromo-(tetrachlorocatecholato-*O*,*O*′)(bis((2-pyridyl)-methyl)-2-pyridylamine-*N*,*N*′,*N*″)-iron(III), (μ-oxo)-bis(bromo)(bis((2-pyridyl)methyl)-2-pyridylamine-*N*,*N*′,*N*″,*N*‴)-diiron-(III), dichloro-((2-(2-pyridyl)ethyl)bis((2-pyridyl)methyl)amine-*N*,*N*′,*N*″,*N*‴)-iron(III) and (tetrachlorocatecholato-O,O′)((2-(2-pyridyl)ethyl)bis((2-pyridyl)methyl)amine-*N*,*N*′,*N*″,*N*‴)-iron(III) are reported.

Introduction

A large variety of mononuclear nonheme iron enzymes are involved in redox processes with molecular oxygen.[1−3] For example, intradiol-cleaving catechol dioxygenases catalyze the insertion of dioxygen into catechols,[3] and during the oxidation reaction, substrates are converted to acyclic *cis,cis*-muconic acid derivatives. Mimicking the structure and function of these enzymes has been an important goal in bioinorganic chemistry during the past decade.[1,4] The crystal structures of a number of complexes of protocatechuate 3,4-dioxygenase (3,4-PCD) from *Pseudomonas putida* reveal an endogenous His_2Tyr_2 donor set,[5−9] and model compounds have been prepared that contained phenolate donor groups. Although such complexes were good structural and spectroscopic models for the active site of 3,4-PCD, they exhibited only poor catechol oxidation abilities. One of the best structural and spectroscopic models to date of the 3,4-PCD site is a model complex, based upon a modified salen ligand, prepared by Fujii and Funahashi.[10]

The first functional models for catechol dioxygenases were reported by Funabiki, who observed catechol cleavage in the presence of an iron salt, pyridine, and bipyridine. However, the nature of the active species involved in the reactions is unknown.[11,12] At present, the most efficient biomimetic model compound for intradiol cleaving catechol dioxygenases is

* To whom correspondence should be addressed. Fax: (+49)-641-9934149 (S.S.); (+49)-251-8338366 (B.K.). E-mail: krebs@uni-muenster.de (B.K.); siegfried.schindler@anorg.chemie.uni-giessen.de (S.S.).

† Dedicated to Professor Rudi van Eldik on the occasion of his 60th birthday.

(1) Costas, M.; Mehn, M. P.; Jensen, M. P.; Que, L., Jr. *Chem. Rev.* **2004**, *104*, 939.
(2) Que, L., Jr.; Ho, R. Y. N. *Chem. Rev.* **1996**, *96*, 2607.
(3) Bugg, T. D. H.; Winfield, C. J. *Nat. Prod. Rep.* **1998**, *15*, 513. Kryatov, S. V.; Rybak-Akimova, E. V.; Schindler, S. *Chem. Rev.* **2005**, *105*, 2175.
(4) Yamahara, R.; Ogo, S.; Masuda, H.; Watanabe, Y. *J. Inorg. Biochem.* **2002**, *88*, 284.
(5) Ohlendorf, D. H.; Lipscomb, J. D.; Weber, P. C. *Nature* **1988**, *336*, 403.
(6) Ohlendorf, D. H.; Orville, A. M.; Lipscomb, J. D. *J. Mol. Biol.* **1994**, *244*, 586.
(7) Orville, A. M.; Lipscomb, J. D.; Ohlendorf, D. H. *Biochemistry* **1997**, *36*, 10052.
(8) Elgren, T. E.; Orville, A. M.; Kelly, K. A.; Lipscomb, J. D.; Ohlendorf, D. H.; Que, L., Jr. *Biochemistry* **1997**, *36*, 11504.
(9) Orville, A. M.; Elango, N.; Lipscomb, J. D.; Ohlendorf, D. H. *Biochemistry* **1997**, *36*, 10039.
(10) Fujii, H.; Funahashi, Y. *Angew. Chem., Int. Ed.* **2002**, *41*, 3638.

10.1021/ic050708k CCC: $30.25
Published on Web 09/23/2005

Scheme 1. Tmpa-Based Ligands with Shortened and Extended Arms

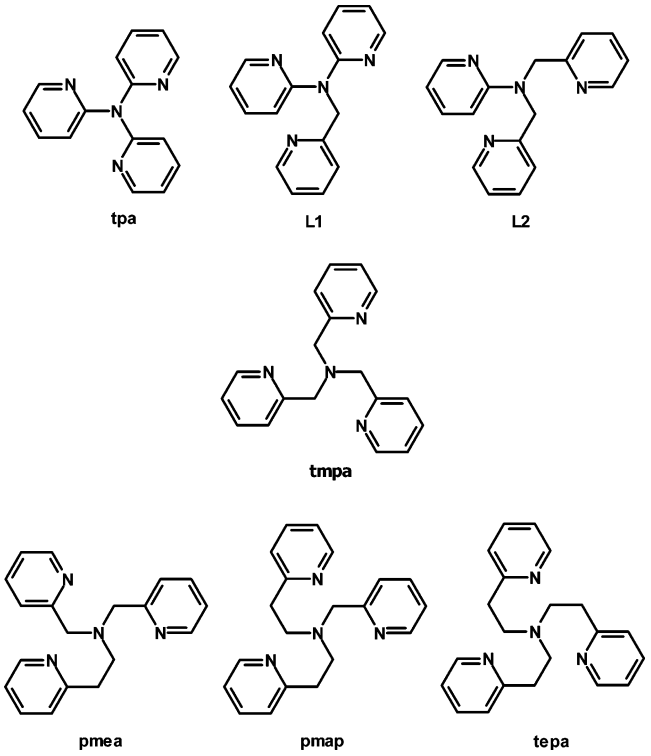

an iron(III) complex of the ligand tris[(2-pyridyl)methyl]-amine (tmpa; also abbreviated as tpa in the literature; Scheme 1), reported by Que and co-workers in 1991.[13]

This result was derived by systematic variation of tetradentate tripodal ligands in which functional groups were changed from phenolate to carboxylate to pyridine in order to alter electron-donating properties of the ligand.[1,14] The resulting change in Lewis acidity of the iron(III) center was observed in the UV−vis−NIR spectra of the complexes. A correlation between the red shift in the LMCT bands of the catecholate complexes and higher catechol dioxygenase activity was observed.[15] In a previous study, we reported that besides electronic effects, the steric demand of the ligands clearly influenced the reactivity of the corresponding iron(III)−catecholate complexes toward dioxygen.[16]

It has been reported previously that variations of the chelate ring size strongly affected the properties of manganese and copper compounds.[17−19] However, to date, no attempt has been made to investigate the properties of iron

Scheme 2. Dianions of Substrates and Inhibitor Substrates Used in This Study and Their Abbreviations

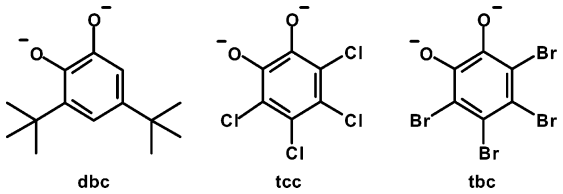

coordination compounds featuring ligands closely related to tmpa, in which the arms of the tripodal ligand have been lengthened or shortened by the insertion or removal of a methylene spacer group (see Scheme 1). Therefore, we describe herein the effect of chelate ring size variations on the coordination chemistry and catechol dioxygenase reactivity of the corresponding iron(III) complexes of the ligands shown in Scheme 1 using the catecholates presented in Scheme 2.

Experimental Section

General Remarks. All chemicals were purchased from commercial sources and used as received. ***CAUTION!*** *The perchlorate salts used in this study are potentially explosive and should be handled with care.*

Physical Measurements. Elemental analyses were carried out on an Elementar vario EL III analyzer. UV−vis spectra were measured at 25.0 °C on a Hewlett-Packard 8453 diode array spectrometer using quarz cuvettes (1 cm).

Stopped-Flow Measurements. Spectroscopic-grade methanol for the kinetic measurements was used without further purification. Preparation and handling of air-sensitive compounds were carried out in a glovebox (M. Braun, Germany). Dioxygen-saturated solutions for the kinetic measurements were prepared by bubbling dioxygen (Linde, Germany) through the solvent for 15 min in a glass syringe with a three-valve stopcock (solubility of dioxygen in methanol is $(8.5 \pm 1.0) \times 10^{-3}$ M at 760 Torr and 25 °C).[20] Varying dioxygen concentrations were obtained by mixing, in appropriate amounts, an oxygen-saturated solution with an argon-saturated solution in syringes. Time-resolved spectra of the reactions of dioxygen with the iron(III) complexes were recorded on a modified Hi-Tech SF-3 L low-temperature stopped-flow unit (Hi-Tech, Salisbury, UK) equipped with a J&M TIDAS 16-500 diode array spectrophotometer (J&M, Aalen, Germany). Data fitting was performed using the integrated J&M software Kinspec, Origin (OriginLab Corporation, Northampton, MA) or Igor (WaveMetrics, Inc., Lake Oswego, OR) for simple exponential functions.

Determination of the Catechol 1,2-Dioxygenase Activity. The catechol-cleaving activities of the complexes prepared in situ in methanol were investigated by adding piperidine as an external base. The amount of base yielding the highest reaction rate possible for each individual complex was determined according to the following spectrophotometric titration: 0.02 mL of a 2×10^{-2} mol L^{-1} (1 equiv) solution of 3,5-H_2dbc (3,5-di-*tert*-butylcatechol) was added to 2 mL of a 2×10^{-4} mol L^{-1} methanolic solution consisting of $Fe(ClO_4)_3 \cdot H_2O$ and the ligand. The determined amount of base (piperidine) was added to the reaction mixture as a 2×10^{-2} mol L^{-1} solution (see Table 1). The decomposition of the complexes was followed at least three times by UV−vis spectroscopy.

Spectrophotometric Titrations. The spectrophotometric titrations were carried out with the same solutions as described above

(11) Funabiki, T.; Sakamoto, H.; Yoshida, S.; Tamara, L. *J. Chem. Soc., Chem. Commun.* **1979**, 754.
(12) Funabiki, T.; Mizoguchi, A.; Sugimoto, T.; Tada, S.; Tsuji, M.; Sakamoto, H.; Yoshida, S. *J. Am. Chem. Soc.* **1986**, *108*, 2921.
(13) Jang, H. G.; Cox, D. D.; Que, L., Jr. *J. Am. Chem. Soc.* **1991**, *113*, 9200−9204.
(14) Cox, D. D.; Que, L., Jr. *J. Am. Chem. Soc.* **1988**, *110*, 8085.
(15) Cox, D. D.; Benkovic, S. J.; Bloom, L. M.; Bradley, F. C.; Nelson, M. J.; Que, L., Jr.; Wallick, D. E. *J. Am. Chem. Soc.* **1988**, *110*, 2026.
(16) Pascaly, M.; Duda, M.; Schweppe, F.; Zurlinden, K.; Müller, F. K.; Krebs, B. *Dalton Trans.* **2001**, 828.
(17) Dietrich, J.; Heinemann, F. W.; Schrodt, A.; Schindler, S. *Inorg. Chim. Acta* **1999**, *288*, 206.
(18) Schatz, M.; Becker, M.; Thaler, F.; Hampel, F.; Schindler, S.; Jacobson, R. R.; Tyeklár, Z.; Murthy, N. N.; Ghosh, P.; Chen, Q.; Zubieta, J.; Karlin, K. D. *Inorg. Chem.* **2001**, *40*, 2312.
(19) Foxon, S. P.; Walter, O.; Schindler, S. *Eur. J. Inorg. Chem.* **2002**, 111.
(20) Battino, R.; Ed. *Oxygen and Ozone*; Solubility Data Series; Pergamon Press: New York, 1981; Vol. 7.

Table 1. Results of the Spectrophotometric Titrations and Catechol-1,2-dioxygenase Activities

ligand	base equivalents needed for optimal catecholate binding	reaction rate constant [$M^{-1}s^{-1}$]
tpa	—[a]	—[b]
L1	—[a]	—[b]
L2	1.3	0.05
tmpa	2.25	10, ref 13
pmea	2.25	0.022
pmap	2.5	0.004
tepa	2.5	—[b]

[a] UV spectra did not show sufficient amounts of the desired $[Fe(L)dbc]^+$ complex during the titration. [b] Complex did not show a significant catechol dioxygenase activity.

for the activity determination. To avoid cleavage of the substrate, all manipulations were carried out under an argon atmosphere. A 0.1 mL sample of the 3,5-H_2dbc solution was added to 10 mL of the complex solution. The resulting solution was titrated with piperidine, and the UV−vis spectra were monitored in a flow cell.

Ligand Syntheses. The ligands tpa,[21] L1,[19] L2,[19] tmpa,[18] pmea,[18,22,23] pmap,[17,18] and tepa[17,18] (see Scheme 1) were synthesized according to methods reported previously.

Syntheses of Complexes. $[Fe(tmpa)(dbc)]B(C_6H_5)_4$ (**1**) was prepared according to a method described previously.[13]

[Fe(L2)(tcc)Br] (2). Tetrachlorocatechol monohydrate (27 mg, 0.1 mmol) was added to a stirred solution of L2 (28 mg, 0.1 mmol) and anhydrous $FeBr_3$ (30 mg, 0.1 mmol) in methanol (8 mL). Triethylamine (28 μL, 20 mg, 0.2 mmol) was then added, and the mixture was heated to reflux for a few seconds and filtered. Vapor diffusion of diethyl ether into the dark blue complex solution yielded needlelike crystals of compound **2** suitable for X-ray analysis. Yield: 32 mg (0.05 mmol, 50%). Anal. Calcd for $C_{23}H_{16}BrCl_4FeN_4O_2$: C, 42.0; H, 2.5; N 8.5. Found: C, 42.2; H, 2.4; N, 8.7. mp: 203 °C (dec).

[(Fe(L2)Br)$_2$O][(FeBr$_3$)$_2$O]·2 CH$_3$OH (3). Anhydrous $FeBr_3$ (30 mg, 0.1 mmol) was added to a stirred solution of L2 (28 mg, 0.1 mmol) in methanol (6 mL). The reaction mixture was heated for a few minutes and filtered. Vapor diffusion of diethyl ether into the complex solution yielded red crystals of compound **3** suitable for X-ray diffraction. Yield: 47 mg (0.03 mmol, 60%). Anal. Calcd for $C_{36}H_{40}Br_8Fe_4N_8O_4$: C, 28.6; H, 2.7; N 7.4. Found: C, 28.9; H, 2.6; N, 7.7. mp: 204 °C (dec).

[Fe(pmea)Cl$_2$]ClO$_4$·(C$_2$H$_5$)$_2$O (4). Anhydrous $FeCl_3$ (16 mg, 0.1 mmol), $Fe(ClO_4)_3 \cdot H_2O$ (19 mg, 0.05 mmol), and pmea (46 mg, 0.15 mmol) were dissolved in acetone (7 mL). The reaction mixture was heated to reflux for a few seconds and filtered. Vapor diffusion of diethyl ether into the complex solution yielded crystalline yellow plates of compound **4** which were suitable for X-ray analysis. Yield: 56 mg (0.09 mmol, 62%). Anal. Calcd for $C_{20.33}H_{23.33}Cl_3FeN_4O_{4.33}$ ($[Fe(pmea)Cl_2]ClO_4 \cdot 1/3(C_2H_5)_2O$): C, 44.0; H, 4.2; N 10.1. Found: C, 44.4; H, 3.9; N, 10.1. mp: 175 °C (dec).

[Fe(pmea)(tbc)]ClO$_4$·H$_2$O (5). $Fe(ClO_4)_3 \cdot H_2O$ (37 mg, 0.1 mmol) and pmea (30 mg, 0.1 mmol) were dissolved in acetone (7 mL). With stirring, tetrabromocatechol (42 mg, 0.1 mmol) and triethylamine (28 μL, 20 mg, 0.2 mmol) were added, changing the color of the solution to dark blue. The reaction mixture was heated and filtered. Vapor diffusion of diethyl ether into the complex solution yielded dark blue crystals of compound **5** that were suitable for X-ray analysis. Yield: 63 mg (0.07 mmol, 70%). Anal. Calcd for $C_{25}H_{20}Br_4ClFeN_4O_7$: C, 34.0; H, 2.3; N 6.2. Found: C, 34.0; H, 2.3; N, 6.4. mp: 218 °C (dec).

X-Ray Crystallographic Studies. The intensity data of **2**−**5** were collected on a Bruker AXS SMART 6000 CCD diffractometer (Cu Kα, λ = 1.54178 Å, Göbel mirror) using an ω-scan technique.

Table 2. Selected Crystallographic Data

compound	**2**	**3**	**4**	**5**
empirical formula	$C_{23}H_{16}BrCl_4FeN_4O_2$	$C_{36}H_{40}Br_8Fe_4N_8O_4$	$C_{23}H_{30}Cl_3FeN_4O_5$	$C_{25}H_{20}Br_4ClFeN_4O_7$
M_r	657.96	1511.44	604.71	901.41
temp [K]	140(2)	130(2)	110(2)	110(2)
radiation (λ [Å])	Cu K$_\alpha$ (1.54178)	Cu K$_\alpha$ (1.54178)	Cu K$_\alpha$ (1.54178)	Cu K$_\alpha$ (1.54178)
cryst shape	rod	rod	Rod	rod
cryst size [mm]	0.25 × 0.08 × 0.03	0.15 × 0.06 × 0.05	0.22 × 0.12 × 0.02	0.20 × 0.10 × 0.07
cryst syst	triclinic	monoclinic	monoclinic	monoclinic
space group	$P\bar{1}$ (No. 2)	$P2_1/c$ (No. 14)	$P2_1/c$ (No. 14)	$P2_1/c$ (No. 14)
a [Å]	7.6179(2)	10.9771(2)	15.7539(4)	9.3253(2)
b [Å]	11.3109(2)	15.4213(2)	12.3338(3)	36.3832(7)
c [Å]	15.1385(3)	15.2598(2)	15.4396(4)	8.6778(2)
α [°]	83.574(1)			
β [°]	88.235(2)	99.740(1)	118.321(2)	92.141(2)
γ [°]	70.800(1)			
V [Å^3]	1224.09(5)	2545.96(7)	2640.9(2)	2942.2(2)
Z	2	2	4	4
ρ_{calcd} [g cm^{-3}]	1.785	1.961	1.521	2.030
μ [mm^{-1}]	11.133	16.674	7.728	11.763
F(000)	654	1456	1252	1756
scan range θ [°]	2.94−71.20	4.09−71.33	3.19−71.30	2.43−71.42
index ranges	$-8 \le h \le 8$	$-10 \le h \le 12$	$-19 \le h \le 16$	$-10 \le h \le 11$
	$-13 \le k \le 13$	$-17 \le k \le 18$	$-14 \le k \le 13$	$-44 \le k \le 41$
	$-16 \le l \le 18$	$-18 \le l \le 16$	$-16 \le l \le 18$	$-10 \le l \le 10$
reflns collected	7149	14 507	14 845	17 053
unique reflns	4066	4714	4872	5414
reflns $I > 2\sigma(I)$	3564	3953	3451	4444
R_{int}	0.0364	0.0418	0.0930	0.0551
data/restraints/params	4066/0/316	4714/0/292	4872/0/327	4486/0/334
GOF on F^2	0.997	1.084	0.943	1.031
final R indices [$I > 2\sigma(I)$]	R1 = 0.0408	R1 = 0.0403	R1 = 0.0482	R1 = 0.0539
	wR2 = 0.1060	wR2 = 0.1114	wR2 = 0.1100	wR2 = 0.1326
R indices (all data)	R1 = 0.0446	R1 = 0.0478	R1 = 0.0716	R1 = 0.0646
	wR2 = 0.1081	wR2 = 0.1142	wR2 = 0.1176	wR2 = 0.1376
largest diff. peak/hole [e Å^{-3}]	0.929/−0.566	1.670/−0.823	0.482/−0.604	1.536/−1.043

Table 3. Selected Bond Lengths [Å] and Angles [deg] for Compounds **2**−**5**

		2			
Fe(1)−Br(1)	2.4525(7)	Br(1)−Fe(1)−O(1)	100.96(8)	O(1)−Fe(1)−N(3)	94.7(2)
Fe(1)−O(1)	1.946(2)	Br(1)−Fe(1)−O(2)	96.95(7)	O(2)−Fe(1)−N(1)	89.6(2)
Fe(1)−O(2)	1.958(2)	Br(1)−Fe(1)−N(1)	167.78(7)	O(2)−Fe(1)−N(2)	88.5(2)
Fe(1)−N(1)	2.398(3)	Br(1)−Fe(1)−N(2)	97.47(8)	O(2)−Fe(1)−N(3)	165.6(2)
Fe(1)−N(2)	2.169(3)	Br(1)−Fe(1)−N(3)	97.45(8)	N(1)−Fe(1)−N(2)	72.3(2)
Fe(1)−N(3)	2.136(3)	O(1)−Fe(1)−O(2)	83.4(2)	N(1)−Fe(1)−N(3)	76.1(2)
O(1)−C(18)	1.322(4)	O(1)−Fe(1)−N(1)	90.0(2)	N(2)−Fe(1)−N(3)	88.9(2)
O(2)−C(23)	1.323(4)	O(1)−Fe(1)−N(2)	160.6(2)		
		3			
Fe(1)−Fe(1A)	3.550(2)	Br(1)−Fe(1)−O(1)	106.8(3)	O(1)−Fe(1)−N(4)	92.5(2)
Fe(1)−Br(1)	2.4046(8)	Br(1)−Fe(1)−N(1)	158.1(2)	N(1)−Fe(1)−N(2)	61.6(2)
Fe(1)−O(1)	1.7747(7)	Br(1)−Fe(1)−N(2)	96.5(2)	N(1)−Fe(1)−N(3)	75.6(2)
Fe(1)−N(1)	2.216(4)	Br(1)−Fe(1)−N(3)	103.9(2)	N(1)−Fe(1)−N(4)	75.7(2)
Fe(1)−N(2)	2.247(4)	Br(1)−Fe(1)−N(4)	102.8(2)	N(2)−Fe(1)−N(3)	83.5(2)
Fe(1)−N(3)	2.172(4)	O(1)−Fe(1)−N(1)	95.1(2)	N(2)−Fe(1)−N(4)	82.9(2)
Fe(1)−N(4)	2.152(4)	O(1)−Fe(1)−N(2)	156.7(2)	N(3)−Fe(1)−N(4)	151.2(2)
		O(1)−Fe(1)−N(3)	90.0(2)		
		4			
Fe(1)−Cl(1)	2.274(2)	Cl(1)−Fe(1)−Cl(2)	98.52(4)	Cl(2)−Fe(1)−N(4)	92.4(8)
Fe(1)−Cl(2)	2.285(2)	Cl(1)−Fe(1)−N(1)	163.98(9)	N(1)−Fe(1)−N(2)	91.9(2)
Fe(1)−N(1)	2.180(3)	Cl(1)−Fe(1)−N(2)	100.01(8)	N(1)−Fe(1)−N(3)	78.1(2)
Fe(1)−N(2)	2.180(3)	Cl(1)−Fe(1)−N(3)	92.66(8)	N(1)−Fe(1)−N(4)	74.5(2)
Fe(1)−N(3)	2.164(3)	Cl(1)−Fe(1)−N(4)	93.07(8)	N(2)−Fe(1)−N(3)	82.8(2)
Fe(1)−N(4)	2.173(3)	Cl(2)−Fe(1)−N(1)	92.22(8)	N(2)−Fe(1)−N(4)	166.3(2)
		Cl(2)−Fe(1)−N(2)	89.72(8)	N(3)−Fe(1)−N(4)	92.6(2)
		Cl(2)−Fe(1)−N(3)	167.49(8)		
		5			
Fe(1)−O(1)	1.927(4)	O(1)−Fe(1)−O(2)	83.4(2)	O(2)−Fe(1)−N(4)	89.1(2)
Fe(1)−O(2)	1.947(4)	O(1)−Fe(1)−N(1)	171.0(2)	N(1)−Fe(1)−N(2)	94.8(2)
Fe(1)−N(1)	2.172(5)	O(1)−Fe(1)−N(2)	90.8(2)	N(1)−Fe(1)−N(3)	76.6(2)
Fe(1)−N(2)	2.148(5)	O(1)−Fe(1)−N(3)	96.1(2)	N(1)−Fe(1)−N(4)	79.1(2)
Fe(1)−N(3)	2.134(5)	O(1)−Fe(1)−N(4)	108.1(2)	N(2)−Fe(1)−N(3)	92.7(2)
Fe(1)−N(4)	2.114(6)	O(2)−Fe(1)−N(1)	91.5(2)	N(2)−Fe(1)−N(4)	88.4(2)
O(1)−C(20)	1.319(7)	O(2)−Fe(1)−N(2)	172.7(2)	N(3)−Fe(1)−N(4)	155.7(2)
O(2)−C(25)	1.326(7)	O(2)−Fe(1)−N(3)	92.4(2)		

The collected reflections were corrected for absorption effects.[24] All structures were solved by direct methods and refined by full-matrix least-squares methods on F^2.[25] Further data-collection parameters are summarized in Table 2. Selected bond lengths and angles for the iron(III) complexes are reported in Table 3. Crystallographic data (excluding structure factors) for the structures reported in this paper have been deposited with the Cambridge Crystallographic Data Centre. Copies of the data can be obtained free of charge on application to the CCDC, 12 Union Road, Cambridge CB2 1EZ, UK, on full quoting of the journal citation and deposition number: CCDC 247601 (**2**), 247602 (**3**), 247603 (**4**), and 247604 (**5**).

Results and Discussion

In an early study, Cox and Que described the reaction of dioxygen with dbc iron(III) complexes using NTA (nitrilotriacetate) and the related ligands PDA (*N*-(2-pyridylmethyl)-iminodiacetate) and BPG (*N*,*N*-bis(2-pyridylmethyl)glycinate).[14] While these oxidations proceeded very slowly, they can be regarded as model reactions for the intradiol cleavage of dioxygenases, and from a kinetic study activation, parameters were obtained. However, when the related tmpa ligand was used, the reaction proceeded much faster and second-order rate constants in DMF and methanol were obtained at 25 °C (15 (DMF) and 10 (MeOH) M^{-1} s^{-1}).[13] In contrast to the other investigated ligands, no temperature-dependence measurements of this system were performed and no activation parameters reported. As pointed out previously by Zuberbühler, for kinetic studies on the reaction of dioxygen with copper(I) complexes, it can be misleading to propose mechanistic arguments on the sole basis of a comparison of kinetic and equilibrium constants at a given temperature rather than on activation and thermodynamic parameters.[26]

A reaction mechanism was proposed for the intradiol cleavage of catechols (Scheme 3).[1] However, the proposed intermediates could not be detected spectroscopically.

Despite efforts to increase the rate of the intradiol cleavage reaction using other ligands, the iron(III) tmpa complex remains, at present, the most active catalyst (some examples are given in the references).[1,27,28] When BPIA[27] ([(1-methylimidazol-2-yl)methyl]bis[(2-pyridyl)methyl]amine, a ligand closely related to tmpa) or L−N_4H_2 [29] (the nonmethylated

(21) Yang, W.; Schmider, H.; Wu, Q.; Zhang, Y.; Wang, S. *Inorg. Chem.* **2000**, *39*, 2397.
(22) Oki, A. R.; Glerup, J.; Hodgson, D. J. *Inorg. Chem.* **1990**, *29*, 2435.
(23) Hoijland, F.; Toftlund, H.; Yde-Anderson, S. *Acta Chem. Scand.* **1983**, *37*, 251.
(24) SADABS *Siemens Area Detector Absorption Correction*; Siemens.
(25) Sheldrick, G. M. *SHELX-97*; Universität Göttingen: Göttingen, Germany, 1997.
(26) Karlin, K. D.; Kaderli, S.; Zuberbühler, A. D. *Acc. Chem. Res.* **1997**, *30*, 139.
(27) Duda, M.; Pascaly, M.; Krebs, B. *Chem. Commun.* **1997**, 835.
(28) Merkel, M.; Schnieders, D.; Baldeau, S. M.; Krebs, B. *Eur. J. Inorg. Chem.* **2004**, 783.

Scheme 3

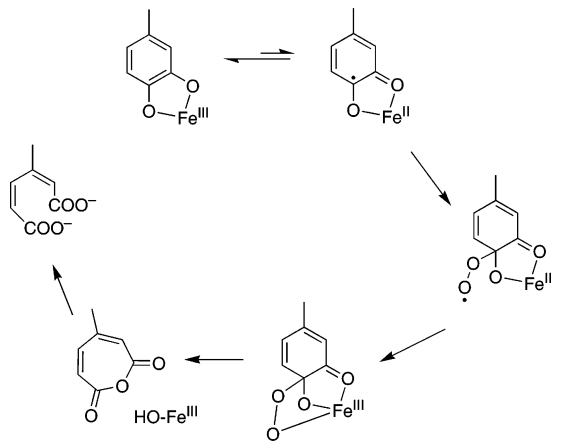

form of tetraazamacrocycle *N*,*N*′-dimethyl-2,11-diaza[3,3]-(2,6)pyridinophane, a ligand thoroughly investigated by Krüger and co-workers)[30] were used as ligands, reaction rates rather close to the tmpa system were observed.

The oxidative cleavage of [Fe(tmpa)(dbc)]B(C_6H_5)$_4$ (**1**) is accompanied by a dramatic change in the UV−vis spectrum. The reaction of dioxygen with **1** in methanol can be followed using low-temperature stopped-flow techniques, and typical time-resolved spectra are presented in Figure 1.

Measurements were performed using pseudo-first-order conditions ([O_2] ≫ [**1**]), and absorbance vs time traces were obtained at different wavelengths that could be fitted to a one-exponential function. Observed rate constants (k_{obs}) at different temperatures showed a linear dependence on the dioxygen concentration (Figure 2) with no intercept, and herewith, the second-order rate law reported previously was confirmed (the published rate constant of 10 M^{-1} s^{-1} at 25 °C[13] was very close, within error, to our determined rate constant).[13]

From the temperature-dependence studies, the activation parameters were calculated using the Eyring equation as $\Delta H^{\ddagger}$ = 23 ± 1 kJ mol^{-1} and $\Delta S^{\ddagger}$ = −199 ± 4 J mol^{-1} K^{-1}. Negative values for the activation entropy were reported for NTA and derivatives (for the NTA complex: $\Delta H^{\ddagger}$ = 12.8

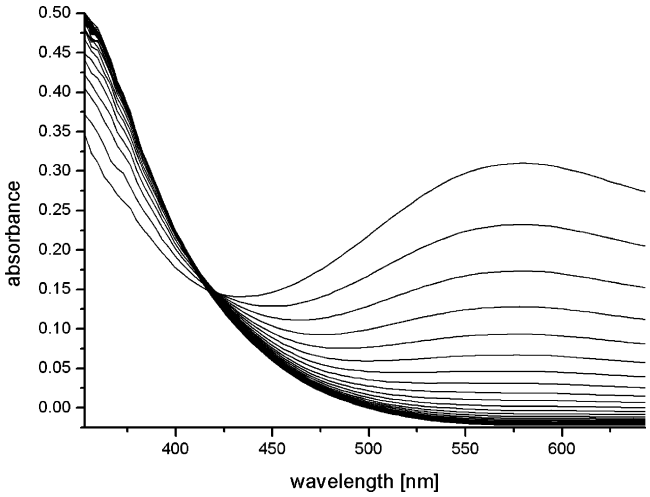

Figure 1. Time-resolved spectra for the reaction of [Fe(tmpa)(dbc)]B(C_6H_5)$_4$ (**1**) (0.16 mmol L^{-1}) with dioxygen (4.25 mmol L^{-1} at 20 °C, total time 153.9 s) in methanol.

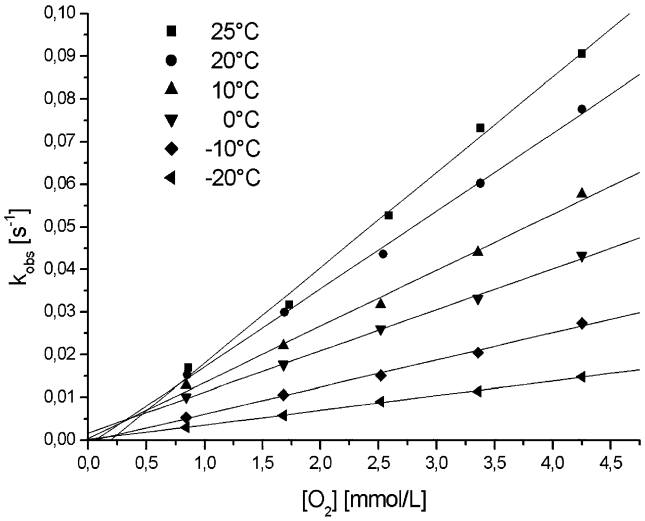

Figure 2. Plot of observed rate constants, k_{obs} (obtained from measurements at 578.0 nm), vs dioxygen concentration at different temperatures.

kcal mol^{-1} and $\Delta S^{\ddagger}$ = −22 eu).[14] As discussed previously, these data are in line with related reactions in copper chemistry[26,31−33] and indicate that the attack of dioxygen on the catecholate complexes is the rate-determining step. However, it is not possible from these data to describe a detailed reaction pathway for this reaction because no intermediates were observed.

Unfortunately, our hope to spectroscopically observe one of the postulated intermediates (Scheme 3) using low-temperature stopped-flow kinetic methods (an approach used successfully in copper dioxygen chemistry) was not fulfilled. Only the UV−vis spectra of the starting complex and the final products were observed. Our kinetic results do not contradict the postulated reaction mechanism (Scheme 3); however, they also do not provide additional evidence for the occurrence of the described reaction steps. The kinetic data support a rate-determining step of the reaction of the catecholate complex with dioxygen. However, at which site this attack takes place cannot be determined in a kinetic study without the observation of intermediates. Furthermore, for the same reason, conclusions in regard to the mechanism of the enzyme should not be drawn from the results of this kinetic study.

Compared to the enzyme, the activity of the tmpa iron(III) complex is still low. Chelate ring size plays an important role in regard to the reactivity of coordination compounds, and so far it has not been investigated for iron(III) complexes of the tmpa system. The ligands shown in Scheme 1 can be readily prepared in good yields by synthetic procedures described previously.

The reactivity of the iron(III) complexes of the ligands depicted in Scheme 1 was investigated (see Table 1). The

(29) Raffard, N.; Carina, R.; Simaan, A. J.; Sainton, J.; Riviere, E.; Tchertanov, L.; Bourcier, S.; Bouchoux, G.; Delroisse, M.; Banse, F.; Girerd, J.-J. *Eur. J. Inorg. Chem.* **2001**, 2249.
(30) Koch, W. O.; Krüger, H.-J. *Angew. Chem.* **1995**, *107*, 2928.
(31) Feig, A. L.; Becker, M.; Schindler, S.; van Eldik, R.; Lippard, S. J. *Inorg. Chem.* **1996**, *35*, 2590.
(32) Becker, M.; Schindler, S.; Karlin, K. D.; Kaden, T. A.; Kaderli, S.; Palanche, T.; Zuberbühler, A. D. *Inorg. Chem.* **1999**, *38*, 1989.
(33) Schindler, S. *Eur. J. Inorg. Chem.* **2000**, 2311.

iron(III) complexes were prepared in situ together with dbc, and their catechol-cleaving activity was determined according to the protocol described in the Experimental Section. Frustratingly, all of the complexes were found to react by orders of magnitude slower than the tmpa system and therefore were not further investigated. The more variations that were made on the original tmpa system, the lower the observed reaction rate constants were. For the ligands L1 and tpa, the reason for the low reaction rates was a low concentration of the desired mononuclear $[Fe(L)dbc]^+$ complexes in solution. The geometric constraints of the ligands may lead to the formation of less-reactive dinuclear species or even triscatecholato iron(III) complexes that are also favored due to the high affinity of catecholates for iron(III) ions.

Similar to related studies on the reaction of dioxygen with copper(I) complexes of the same ligands,[18,19] increasing or decreasing chelate ring sizes in the iron(III) complexes (compared to the tmpa system) causes a dramatic decrease in the reactivity of these compounds (the larger the changes, the larger the decrease in reactivity).

Control experiments with just iron(III) perchlorate, 4.5 equiv of piperidine, and 1 equiv of H_2dbc revealed only negligible decay of the formed catecholate complexes over a period of days. Furthermore, Funabiki et al. reported that in oxygenation reactions that utilized a mixture of bipyridine and pyridine as ligands, the main product was the simple oxidation product, 3,5-di-*tert*-butylquinone.[12] For the reason of comparison with other systems, piperidine was used as a base in all reactivity studies reported herein (no reactivity differences were observed with triethylamine instead of piperidine; triethylamine was used in the syntheses of the complexes reported below).

Iron(III) tmpa complexes[13,34,35] and an iron(II) complex of tpa[36] have been prepared and structurally characterized. However, no crystal structures of the iron(III) complexes of the other ligands (depicted in Scheme 1) have been reported. Therefore, iron(III) complexes of the ligands (depicted in Scheme 1) were isolated as solids, and crystals suitable for X-ray structural analysis were obtained for iron(III) complexes of the ligands L2 and pmea with and without catecholate as additional ligands.

[Fe(L2)(tcc)Br] (2). Compound **2** crystallizes in the triclinic space group $P\bar{1}$ with two molecules per unit cell. The structure of the neutral complex is depicted in Figure 3, while selected bond lengths and angles are given in Table 3. The iron(III) center is surrounded by a distorted octahedral N_3O_2Br environment. As reported for copper(II) complexes of the ligand L2,[19] the shorter arm is not coordinated to the metal center, avoiding the formation of a strained four-membered chelate ring which leads to a facial coordination mode for L2 in complex **2**. The catecholate oxygens [O(1) and O(2)] and the bound pyridine nitrogen donors of L2 [N(2) and N(3)] occupy the equatorial plane of the coordination octahedron, whereas the apical sites are occupied by the bromide anion and nitrogen donor N(1) of the tripodal ligand.

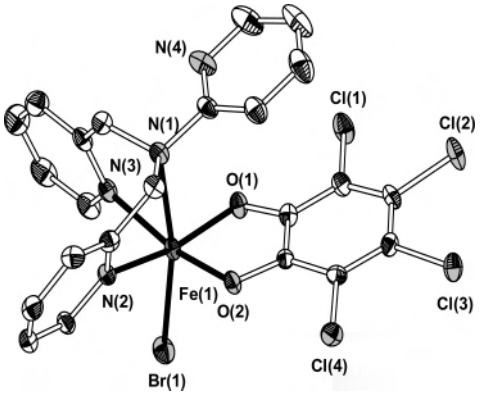

Figure 3. Ellipsoid plot of [Fe(L2)(tcc)Br] (50% probability ellipsoids); hydrogen atoms omitted for clarity.

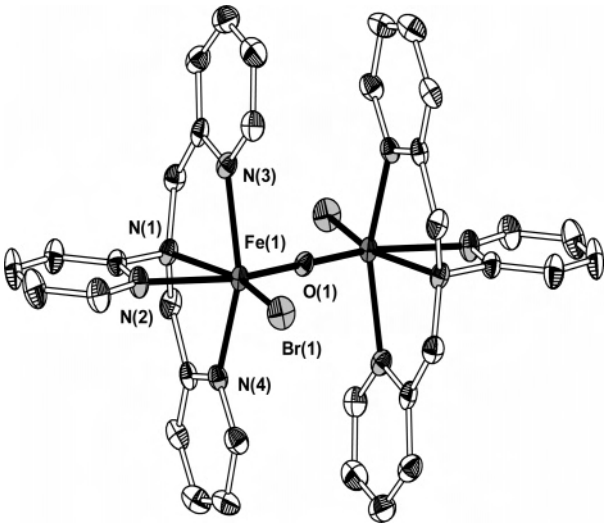

Figure 4. Ellipsoid plot of $[(Fe(L2)Br)_2O]^{2+}$ (50% probability ellipsoids); hydrogen atoms omitted for clarity.

The iron(III) donor bond lengths reveal a stretching of the coordination octahedron along the N(1)−Fe(1)−Br(1) axis. The uncommon length of the Fe(1)−N(1) bond [2.398(3) Å] can be attributed to both the lack of π-donor abilities of the aliphatic amine nitrogen N(1) and to a trans influence of the opposing bromo ligand. The distorted octahedral geometry is also reflected in the bond angles around the iron(III) center; the bite angles involving the five-membered chelate rings of L2 are significantly reduced from 90° [83.4(2)° for O(1)−Fe(1)−O(2), 72.3(2)° and 76.1(2)° for N(1)−Fe(1)−N(2/3)], whereas the cis angles incorporating the bromide anion are significantly larger than 90° because of its steric demand and electrostatic repulsions.

$[(Fe(L2)Br)_2O][(FeBr_3)_2O]\cdot 2\ CH_3OH$ (3). Compound **3** crystallizes in the monoclinic space group $P2_1/c$ with two complex cations, two complex anions, and four disordered methanol molecules per unit cell. The structure of the cationic metal complex is depicted in Figure 4, while selected bond lengths and angles are given in Table 3. The bridging μ-oxo

(34) Merkel, M.; Pascaly, M.; Wieting, M.; Duda, M.; Rompel, A. *Z. Anorg. Allg. Chem.* **2003**, *629*, 2216.
(35) Kojima, T.; Leising, R. A.; Shiping, Y.; Que, L., Jr. *J. Am. Chem. Soc.* **1993**, *115*, 11328.
(36) Kucharski, E. S.; McWhinnie, W. R.; White, A. H. *Aust. J. Chem.* **1976**, *31*, 53.

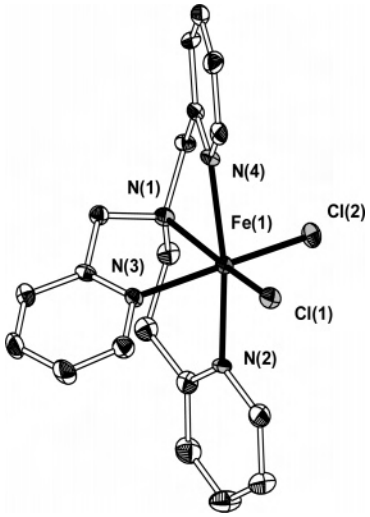

Figure 5. Ellipsoid plot of $[Fe(pmea)Cl_2]^+$ (50% probability ellipsoids); hydrogen atoms omitted for clarity.

group of the $[(Fe(L2)Br)_2O]^{2+}$ cation and that of the $[(FeBr_3)_2O]^{2-}$ anion are located on crystallographic centers of inversion so that one-half of each complex is symmetry generated. The iron(III)···iron(III) distance in the cation is 3.550(2) Å.

The remaining coordination sites of the iron(III) center are occupied by the μ-oxo bridge and a bromide anion, resulting in an N_4BrO donor set around each iron(III) center. The most striking feature of the dinuclear complex **3** is that all three pyridyl groups of L2 are bound to the iron(III) center, which is in stark contrast to all other known metal complexes of L2. As a consequence, the very small bite angle of 61.6(2)° for N(1)−Fe(1)−N(2) is observed. The high tension of the four-membered chelate ring and the trans influence of the opposing μ-oxo bridge weaken the Fe(1)−N(2) bond [2.247(4) Å], which is, despite the possibility of π-bonding, even longer than the Fe(1)−N(1) bond [2.216(4) Å]. The other cis angles that are formed by the ligand and the iron(III) center are also significantly distorted from 90°; [N(1)−Fe(1)−N(3) = 75.6(2)° and N(1)−Fe(1)−N(4) = 75.7(2)°]. The steric demand of the bromide anion increases the Br−Fe−N/O angles. Due to the electrostatic repulsions between Br(1) and O(1), these donors form the largest cis angle found around the iron(III) center [Br(1)−Fe(1)−O(1) = 106.83(3)°]. Such a large angle is enabled by the small opposing angle N(1)−Fe(1)−N(2) (vide infra).

$[Fe(pmea)Cl_2]ClO_4\cdot(C_2H_5)_2O$ (4). Compound **4** crystallizes in the monoclinic space group $P2_1/c$ with four complex cations, four perchlorate counterions, and four diethyl ether molecules per unit cell. An ellipsoid plot of the cation's structure is depicted in Figure 5, with selected bond lengths and angles in Table 3. The coordination geometry around the iron(III) center Fe(1) is best described as distorted octahedral with an N_4Cl_2 donor set. The equatorial plane around Fe(1) consists of two chloride anions Cl(1) and Cl(2), the pyridyl donor atom N(3), and the amine donor atom N(1) of the ligand pmea. The apical sites are occupied by the pyridyl donors N(2) and N(4) with the two five-membered chelate rings located cis to each other.

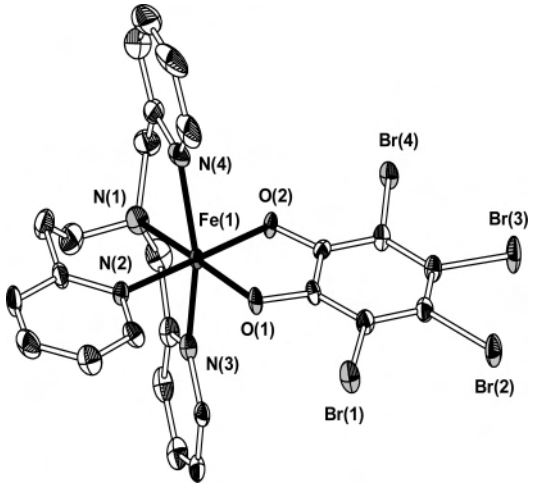

Figure 6. Ellipsoid plot of $[Fe(pmea)(tbc)]^+$ (50% probability ellipsoids); hydrogen atoms omitted for clarity.

The largest cis angle within complex **4** is Cl(1)−Fe(1)−Cl(2) = 98.52(4)°. The rigid five-membered chelate rings of pmea cause a strong distortion of the octahedral coordination sphere around the iron(III) center, with the following angles deviating from 90°: [N(1)−Fe(1)−N(3) = 78.1° and N(1)−Fe(1)−N(4) = 74.5(2)°]. In contrast, the six-membered chelate ring in complex **4** is more flexible and the angle N(1)−Fe(1)−N(2) has an almost ideal value of 91.9(2)°. The coordination of the two chloride anions leads to an expansion of the equatorial plane in their direction, with the corresponding bond lengths being about 0.1 Å longer than the average Fe−N bond in complex **4**. Furthermore, the Fe−Cl bonds show a slight trans influence derived from the different nature of the opposing donors; the longer Fe(1)−Cl(2) bond is trans to the stronger Fe(1)−N(3) bond of a pyridine donor, while the shorter Fe(1)−Cl(1) bond is located vis-à-vis to the weaker Fe(1)−N(1) bond of the aliphatic amine.

$[Fe(pmea)(tbc)]ClO_4\cdot H_2O$ (5). Compound **5** crystallizes in the monoclinic space group $P2_1/c$ with four complex cations, four perchlorate counterions, and four water molecules per unit cell. Each of the water molecules is hydrogen-bonded to one perchlorate ion. The structure of the cation in **5** is depicted in Figure 6, selected bond lengths and angles are listed in Table 3.

As observed for the iron complex **4**, the coordination geometry around the iron(III) center is distorted octahedral. The nitrogen donor atoms of the N_4O_2 donor set are provided by the ligand pmea, while the oxygen donors derive from a tetrabromocatecholate dianion (tbc) that acts as an inhibitor substrate. The equatorial plane around Fe(1) is occupied by O(1) and O(2) of the tbc, the aliphatic nitrogen N(1), and the pyridyl donor N(2) of the extended ligand arm which forms the six-membered chelate ring. This is in contrast to precursor complex **4**, where this arm was located in an apical position. Within this equatorial plane, the deviations from the ideal geometry are relatively small for a metal complex of a tmpa-type ligand. Large deviations can be found for the angles that span the apical positions: [N(1)−Fe(1)−N(3) = 76.6(2)° and N(1)−Fe(1)−N(4) = 79.1(2)° are narrowed, whereas O(1)−Fe(1)−N(3) = 96.1(2)° and O(1)−Fe(1)−

N(4) = 108.1(2)° are widened significantly]. The Fe−N bond lengths are within the typical range for a high-spin iron(III) complex. As expected, the Fe(1)−N(1) bond is the longest Fe−N bond in **5** due to the lack of π-bonding abilities. The binding of the catecholate is slightly asymmetric, but the Fe−O bond lengths, as well as those of the corresponding C−O bonds, are still in good agreement with a dianionic binding of the inhibitor substrate.

Comparative Discussion. In the following, the structures of the metal complexes **2** and **3** will be compared to the complexes $[Fe(tmpa)Cl_2]^+$ (**A**) and $[Fe_2OCl_2(tmpa)_2]^{2+}$ (**B**) that were crystallized by Que and co-workers.[35] Furthermore, structural aspects of the substrate-bound iron(III) complexes $[Fe(pmea)(tbc)]^+$ (cation of **5**) and $[Fe(tmpa)(dbc)]^+$ (**1**)[13] will be discussed.

Ligand L2 is a derivative of tmpa in which one ligand arm lacks a methylene spacer between the central amine group and the pyridyl group. This variation has dramatic effects on the coordination chemistry of L2. Not only have different bond lengths and angles been observed for the primary coordination sphere of the iron(III) center, but also the coordination mode of the ligand was found to be tridentate in the mononuclear substrate complex **2** and tetradentate in the dinuclear compound **3**, whereas tmpa acts as a tetradentate ligand in both **A** and **B**. The very small N(1)−Fe(1)−N(2) angle of 61.6(2)° in **3** compared to 76.8° for the corresponding angle in **B** is indicative of the high ring tension that leads to the detachment of the pyridyl group of L2 upon substrate binding.

The complexes $[Fe(tmpa)(dbc)]^+$ (**1**) and $[Fe(pmea)(tbc)]^+$ (**5**) show a wide similarity; however, there are differences that might explain the lower reactivity of the pmea complex toward dioxygen. A calculation of the angle between the least-squares planes of the catecholate unit and the equatorial pyridine group of the ligand in **1** and **5** was performed. In **5**, this angle has a value of 1.5° and the corresponding groups are nearly coplanar, while in **1**, the dihedral angle has a value of 35.0° due to the ligand's geometric constraints. The twist of the pyridyl group has an impact on the overlap of the ligand's π-orbital with the metal's d orbitals and thus influences the electronic properties of the metal center. Another difference can be observed for the $Fe-O_{cat}$ bond lengths which are both more than 0.03 Å longer in **5** than in **1** [1.917(3) and 1.898(2) Å, respectively]. Since this discrepancy might be a result of the different catechol substrates used in these complexes, we will not go into detail on this point. However, a higher covalency of these bonds that leads to shorter Fe−O distances would simplify charge transfer from the catecholate to the metal center and thereby enhance reactivity toward dioxygen. The slight asymmetry in the substrate binding that was found in **1** (the Fe−O bonds differ by about 0.02 Å) can also be observed in the catecholate complexes in this work (ΔFe−O = 0.01 or 0.02 Å for **2** and **5**, respectively).

Summary

Activation parameters for the reaction of dioxygen with $[Fe(tmpa)(dbc)]B(C_6H_5)_4$ were determined by low-temperature stopped-flow kinetics. The large negative value of $\Delta S^{\ddagger}$ (-199 ± 4 J mol^{-1} K^{-1}) indicated an associative character of the reaction. However, no intermediates could be detected during the oxidation process to support the postulated mechanism outlined in Scheme 3. Furthermore, we could clearly demonstrate that chelate ring size modification in the iron tmpa catecholate system decreased the reaction rate dramatically. In our efforts to crystallize iron catecholate complexes of all ligands investigated, we succeeded in structurally characterizing complexes with the ligands L2 and pmea. Single-crystal X-ray structure analyses of complexes **2** and **3** showed that either all pyridine nitrogen atoms of ligand L2 are coordinated (leading to one four-membered chelate ring in complex **3**) or as for complex **2** one arm of L2 is replaced by an additional ligand.

Acknowledgment. We thank the Deutsche Forschungsgemeinschaft and the Fonds der Chemischen Industrie for financial support. M.M. thanks the University of Münster and the International Graduate College "Template Directed Chemical Synthesis" for graduate fellowships. S.S. thanks Prof. Dr. Rudi van Eldik (University of Erlangen-Nürnberg for support at the beginning of this work).

IC050708K